GPS Solutions (2018) 22:54
https://doi.org/10.1007/s10291-018-0719-9

ORIGINAL ARTICLE

Design and validation of broadcast ephemeris for low Earth orbit satellites

Xin Xie[1] · Tao Geng[1,2] · Qile Zhao[1,2] · Xianglin Liu[3] · Qiang Zhang[1] · Jingnan Liu[1,2]

Received: 20 December 2017 / Accepted: 20 March 2018

Abstract
Low Earth orbit (LEO) constellations have potentialities to augment global navigation satellite systems for better service performance. The prerequisite is to provide the broadcast ephemerides that meet the accuracy requirement for navigation and positioning. In this study, the Kepler ephemeris model is chosen as the basis of LEO broadcast ephemeris design for backward compatibility and simplicity. To eliminate the singularity caused by the smaller eccentricity of LEO satellites compared to MEO satellites, non-singular elements are introduced for curve fitting of parameters and then transformed to Kepler elements to assure the algorithm of ephemeris computation remains unchanged for the user. We analyze the variation characteristics of LEO orbital elements and establish suitable broadcast ephemeris models considering fit accuracy, number of parameters, fit interval, and orbital altitude. The results of the fit accuracy for different fit intervals and orbital altitudes suggest that the optimal parameter selections are ($Crs3, Crc3$), ($Crs3, Crc3, \dot{a}, \dot{n}$) and $\left(Crs3, Crc3, \dot{a}, \dot{n}, \ddot{i}, \ddot{a}\right)$, i.e., adding two, four or six parameters to the GPS 16-parameter ephemeris. When adding four parameters, the fit accuracy can be improved by about one order of magnitude compared to the GPS 16-parameter ephemeris model, and fit errors of less than 10 cm can be achieved with 20-min fit interval for a 400–1400 km orbital altitude. In addition, the effects of the number of parameters, fit interval, and orbit altitude on fit accuracy are discussed in detail. The validation with four LEO satellites in orbit also confirms the effectiveness of proposed models.

Keywords LEO satellites navigation · Broadcast ephemeris · Kepler ephemeris model · Non-singular orbital elements · Least squares curve fit

Introduction

Current global navigation satellite systems (GNSSs) like GPS, GLONASS, and Galileo utilize satellites in medium Earth orbit (MEO) and transmit navigation signals in the microwave band. The constellation of the Chinese GNSS BeiDou consists of geostationary orbit (GEO), inclined geostationary orbit (IGSO), and MEO satellites. Regional navigation satellite systems such as the Japanese Quasi-Zenith Satellite System (QZSS) and the Indian Regional Navigation Satellite System (IRNSS) transmit navigation signals using a constellation of IGSO and GEO satellites, which aim to provide or enhance a regional service. In addition, satellite-based augmentation systems (SBAS) enhance the positioning performance of GNSS by providing integrity and correction information transmitted from GEO satellites. The American Wide Area Augmentation System (WAAS) and the European Geostationary Navigation Overlay System (EGNOS) are such SBAS examples. The missing orbit class is low Earth orbit (LEO), where the majority of operational satellites reside with altitudes of 300–1500 km (Montenbruck and Gill 2000), that is not yet used for transmitting either navigation signals or integrity and correction information.

In recent years, some companies such as OneWeb, SpaceX, and Boeing announced to build commercial broadband LEO constellations of hundreds or even thousands of satellites, aiming at delivering broadband Internet globally. Reid et al. (2016) proposed such LEO constellations can

✉ Tao Geng
gt_gengtao@whu.edu.cn

[1] GNSS Research Center, Wuhan University, 129 Luoyu Road, Wuhan 430079, China

[2] Collaborative Innovation Center of Geospatial Technology, 129 Luoyu Road, Wuhan 430079, China

[3] Fugro Intersite B.V., 2263 HW Leidschendam, The Netherlands

Published online: 26 March 2018

be leveraged as a platform to provide navigation services and demonstrated the feasibility of LEO satellites navigation with respect to user geometry, user range error (URE), and hosted payload concept by simulation. By virtue of the low altitudes, the LEO satellites experience less free-space loss than current GNSS satellites and thus deliver a stronger signal to the Earth, which makes them more resilient to jamming (Rabinowitz and Spilker 2005). In addition, the large geometric variations from fast-moving LEO satellites enable rapid convergence of carrier phase ambiguities (Joerger et al. 2010; Tian et al. 2014). Integrating LEO constellations into the GNSS system gives rise to the possibility for real-time, high-precision, and robust carrier phase positioning over wide areas (Joerger et al. 2009, 2010). A key element for each satellite navigation system is the ability to broadcast ephemeris messages, which provide users the position and velocity of the satellites, enabling meaningful ranging and ultimately positioning.

The broadcast ephemeris parameters are generally produced by the Control Segment via a least squares curve fit of the predicted ephemeris. The legacy navigation (LNAV) message of the GPS broadcast ephemeris is based on the Kepler ephemeris model, which is also used in Galileo, BeiDou, and QZSS constellations (CSNO 2013; GPS Directorate 2013; EU 2015; JAXA 2014). It consists of 16 parameters that describe the satellite orbit. To achieve higher-accuracy orbital representations, two extra parameters for the semimajor axis rate and the mean motion rate are considered in the new civil navigation (CNAV) message transmitted with the L2 and L5 signals of GPS and QZSS (Yin et al. 2015). Typical update interval of broadcast ephemerides for GPS LNAV, GPS CNAV, BeiDou, Galileo, and QZSS is 2, 3, 1 h, 10–180, and 15 min, respectively (Hugentobler and Montenbruck 2017). In addition, the Cartesian ephemeris model, including the position, velocity, and residual acceleration mainly due to lunisolar attraction in the Earth-centered Earth-fixed (ECEF) coordinate system, is used for GLONASS orbital representations with an updating rate of 30 min (ICD-GLONASS 2016). The computation of GLONASS satellite position requires numerical integration, which is more complex than the user algorithm of GPS. The ephemeris parameters of SBAS are similar to GLONASS. However, only a simple quadratic polynomial interpolation is used to compute satellite position of SBAS due to a short update interval of about 4 min (JAXA 2014). The quality of the broadcast ephemeris data is driven by model fit errors and orbit determination as well as propagation errors. The overall broadcast orbit error has been assessed in various studies (Heng et al. 2011; Hu et al. 2013; Warren and Raquet 2003). Montenbruck et al. (2014) demonstrated the orbit-only contribution to the URE in the year 2014 was about 0.24, 0.54, 0.76, 0.50, and 0.57 m for GPS, GLONASS, Galileo, QZSS, and BeiDou IGSO and MEO satellites, respectively. For the model fit error, the root mean square (RMS) of fitted URE is about 5–10 cm for MEO satellites with 4-h fit interval (Diesposti et al. 2004; Fu and Wu 2011).

Research on broadcast ephemeris representations has mainly focused on MEO, IGSO, and GEO, which include the design of broadcast ephemeris parameters (Reid et al. 2015; Dierendonck et al. 1978), the algorithm of ephemeris interpolation and curve fitting (He et al. 2014; Horemuž and Andersson 2006), and the comparison of different ephemeris models (Diesposti et al. 2004; Du et al. 2014). It is necessary to carry out similar studies for LEO broadcast ephemeris. Compared to MEO, IGSO, and GEO satellites, since the LEOs are closer to the Earth they have a very short orbital period and are more affected by higher-order gravity terms and atmospheric drag. As such, the orbit dynamics of LEOs is more complex. The broadcast ephemeris of the now-retired Navy Navigation Satellite System (TRANSIT) contains two parts, one is defined by Kepler-style elements with the update rate of 12 h, and the other is a set of corrections at each 2-min time point (Thomas and Stansell 1968). The model fit error for the orbital representation is about 5 m (Piscane et al. 1973). Such an ephemeris model has no advantage compared to GPS-type broadcast ephemeris in terms of accuracy and simplicity. Reid et al. (2016) used GPS LNAV broadcast ephemeris parameters to fit LEOs of 400–1400 km altitude with different fit intervals; the results demonstrated that a fit interval of 10–20 min is required to match GPS 4-h fit accuracy. An extended GLONASS ephemeris model with 21 parameters is used in Fang et al. (2016) to fit LEOs; the fit errors of a 1000 km orbit with 20-min fit interval for along-track, cross-track, and radial components are 0.161, 0.162, and 0.019 m, respectively. Moreover, it is desirable that the ephemeris model used in LEO is the same as that used by most GNSSs for reasons of compatibility, which is the Kepler ephemeris model. However, as a result of the small eccentricity for LEO satellites, the Kepler orbital elements are usually singular. Du et al. (2014) used non-singular elements to remove the singularities caused by small inclination and small eccentricity in representing BeiDou GEOs, but the algorithm of satellites position computation is much more complex than that for GPS-type broadcast ephemeris.

In this study, we introduce non-singular elements suitable for LEOs, which can be easily transformed to Kepler elements. In this way, the user algorithm remains essentially unchanged compared to the GPS-type ephemeris model. To improve the fit accuracy of LEOs, the modified ephemeris parameter sets are particularly designed by adding a few parameters on the basis of GPS LNAV ephemeris. After presenting the non-singular elements for LEO and analyzing their characteristics, we describe the design and computation of ephemeris parameters. In the subsequent section, we show our results of fit accuracy and parameter selection

for different numbers of parameters. Finally, we discuss the effects of the number of parameters, fit interval, and orbital altitude on fit results and verify the proposed ephemeris model by real LEOs.

Non-singular elements for LEO

The motion of a satellite in orbit is usually described through the six Kepler elements $(a, e, i, \Omega, \omega, M)$. They represent the semimajor axis, eccentricity, inclination, right ascension of the ascending node (RAAN), the argument of perigee, and mean anomaly, respectively.

However, the Kepler orbital elements have singularities at the eccentricity and inclination close to zero (Xu and Xu 2013). Various non-singular element sets have been applied to eliminate the singularity (Hintz 2008; Montenbruck and Gill 2000). The great majority of LEO satellites are chosen to be in near-circular orbits, and the singularity is mainly caused by small eccentricity, where the time derivatives of ω and M contain a singularity at $e = 0$ (Xu and Xu 2007). To overcome this problem, a non-singular element set $(a, i, \Omega, e_x, e_y, \lambda)$ is selected in this study for LEO ephemeris parameters fitting, with

$$e_x = e\ \cos\omega, \quad e_y = e\ \sin\omega, \quad \lambda = \omega + M \tag{1}$$

where λ eliminates the problem of the small denominator for the time derivatives of ω and M.

The above non-singular elements can be easily transformed to classical Kepler elements as,

$$e = \sqrt{e_x^2 + e_y^2}, \quad \omega = \arctan(e_y/e_x), \quad M = \lambda - \omega \tag{2}$$

As such, what is broadcast to the user are still Kepler elements, and the user algorithm remains unchanged.

Aside from the central force of the Earth, various forces such as the non-central force, the solar and lunar attractions, the atmosphere drag, as well as solar radiation pressure cause orbital perturbations (Brouwer et al. 2005; Gilthorpe and Moore 1992). The perturbations in satellite orbits induce typical variations in Kepler elements or non-singular elements. These can be classified into short-periodic, long-periodic, and secular variations. In order to assess the impact of perturbing forces on LEOs, the characteristics of orbital elements variations need to be studied. Representative results are presented in Fig. 1. The left panels show the time variations of six non-singular elements of satellite HY-2A (Guo et al. 2015) for 1 day. The altitude of HY-2A satellite is about 970 km and corresponds to an orbital period of about 104.5 min. The periodicity of these elements can be found in the right panels, which show the amplitude spectrum of corresponding elements for a time period of 1 week. The

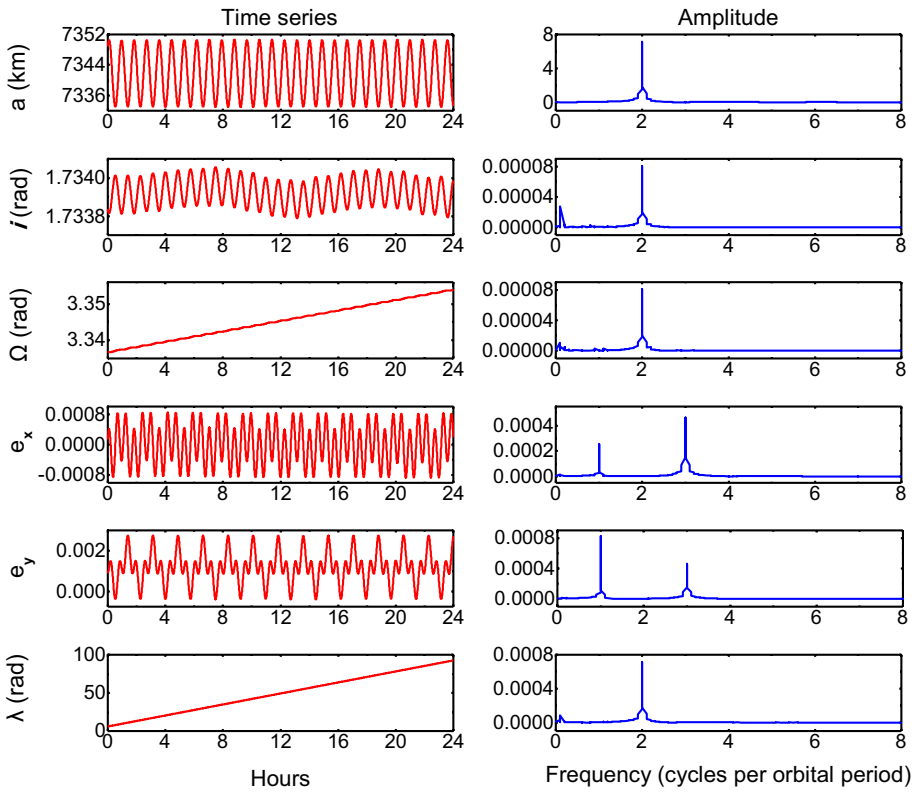

Fig. 1 Time variations over 1 day (left) and the amplitude spectrum over 1 week (right) for six non-singular elements $(a, i, \Omega, e_x, e_y, \lambda)$ of satellite HY-2A at an altitude of about 970 km

secular variations have been removed by polynomial fitting before the spectrum analysis.

In Fig. 1, the semimajor axis (a) shows short-periodic oscillations with a period equivalent to half a revolution. The variation of the inclination (i) contains a short-periodic term and a long-periodic one. The RAAN (Ω) and λ show a secular perturbation superimposed by a short-periodic variation with a period equivalent to half a revolution. The elements e_x and e_y show short-periodic variations consisting of a superposition of once-per-revolution oscillation and three-times-per-revolution oscillation.

LEO ephemeris parameters design

Due to perturbations, the six osculating Kepler elements are not enough to achieve the required orbit accuracy for navigation (Montenbruck and Gill 2000). The GPS LNAV ephemeris contains nine additional correction terms to compensate dominant perturbation forces and represent the variations in orbital elements, as listed in Table 1. This includes six second-order harmonic correction terms ($Cus2, Cuc2, Crs2, Crc2, Cis2, Cic2$) which account for the short-periodic variations with a characteristic of twice the orbital period, and three rate terms ($\Delta n, \dot{i}, \dot{\Omega}$) to capture the secular and long-periodic variations, as listed in Table 1.

For LEO satellites, the accuracy of orbital representations using 16 parameters is significantly worse than for GNSS satellites within the same interval, due to a short period and more complex dynamics. As such, some additional parameters are considered for addition to the 16 GPS parameters to improve accuracy and for backward compatibility. According to analysis of the characteristics of the orbital elements, the first-order and third-order harmonic parameters are considered as the candidates to account for short-periodic variations. As a pair, cosine and sine harmonic parameters of the same order and the same orbital element should simultaneously be either selected or not. The semimajor axis rate ($\dot{a}$) and the mean motion rate ($\dot{n}$) are also considered, which is equivalent to GPS CNAV ephemeris parameters. In addition, the second-order rates ($\ddot{a}, \ddot{n}, \ddot{i}, \ddot{\Omega}$) of semimajor axis, mean motion, inclination, and RAAN are also included to provide possible options for describing in depth the linear variations of these elements. All optional parameters are listed in Table 1. In this study, we only consider the situations for selecting two, four, and six parameters from these candidates to be added to the GPS LNAV parameters.

User algorithm

The user shall compute the satellite position in the ECEF coordinate system utilizing a user algorithm, which is the foundation of broadcast ephemeris parameters curve fitting. The detailed ephemeris computation process for GPS LNAV and CNAV message can be found in GPS Interface Control Documents (GPS Directorate 2013). Herein, the optional parameters listed in Table 1 are also considered, even though only a few of them shall be chosen. The satellite position at epoch t can be computed as follows:

$$a = \left(\sqrt{a}\right)^2 + \dot{a}(t - t_e) + \frac{1}{2}\ddot{a}(t - t_e)^2 \tag{3}$$

$$n = \sqrt{\frac{GM_{\oplus}}{a^3}} + \Delta n + \dot{n}(t - t_e) + \frac{1}{2}\ddot{n}(t - t_e)^2 \tag{4}$$

The mean anomaly (M), eccentric anomaly (E), and true anomaly (ν) can then be computed by

$$M = M_0 + n(t - t_e) \tag{5}$$

$$E = M + e\ \sin E \tag{6}$$

$$\nu = 2\tan^{-1}\left(\frac{\sqrt{1+e}}{\sqrt{1-e}}\tan\frac{E}{2}\right) \tag{7}$$

Then, one can obtain the uncorrected argument of latitude ($\bar{u}$)

$$\bar{u} = \omega + \nu \tag{8}$$

The short-periodic corrections to argument of latitude (u), radius (r) and inclination (i) can be computed

Table 1 GPS LNAV ephemeris parameters and additional parameters for selection

	GPS LNAV parameters	Optional parameters
Reference epoch	te	–
Orbital elements	$\sqrt{a}, e, i_0, \Omega_0, \omega, M_0$	–
Short-periodic correction	$Cus2, Cuc2, Crs2, Crc2, Cis2, Cic2$	$Cus1, Cuc1, Crs1, Crc1, Cis1, Cic1$ $Cus3, Cuc3, Crs3, Crc3, Cis3, Cic3$
Long-periodic and secular correction	$\Delta n, \dot{\Omega}, \dot{i}(idot)$	$\dot{a}, \dot{n}, \ddot{a}, \ddot{n}, \dddot{i}, \dddot{\Omega}$

$$\begin{aligned}\delta u &= Cus1\sin(\bar{u}) + Cuc1\cos(\bar{u}) + Cus2\sin(2\bar{u}) + Cuc2\cos(2\bar{u}) + Cus3\sin(3\bar{u}) + Cuc3\cos(3\bar{u})\\ \delta r &= Crs1\sin(\bar{u}) + Crc1\cos(\bar{u}) + Crs2\sin(2\bar{u}) + Crc2\cos(2\bar{u}) + Crs3\sin(3\bar{u}) + Crc3\cos(3\bar{u})\\ \delta i &= Cis1\sin(\bar{u}) + Cic1\cos(\bar{u}) + Cis2\sin(2\bar{u}) + Cic2\cos(2\bar{u}) + Cis3\sin(3\bar{u}) + Cic3\cos(3\bar{u})\end{aligned} \tag{9}$$

and the perturbed values of these elements are obtained,

$$\begin{aligned}u &= \bar{u} + \delta u\\ r &= a(1 - e\cos E) + \delta r\\ i &= i_0 + \delta i + \dot{i}(t - t_e) + \tfrac{1}{2}\ddot{i}(t - t_e)^2\end{aligned} \tag{10}$$

In addition, the longitude of the ascending node is given by

$$\lambda_\Omega = \Omega_0 + \dot{\Omega}(t - t_e) + \frac{1}{2}\ddot{\Omega}(t - t_e)^2 - \Theta \tag{11}$$

where $\Theta = \omega_\oplus(t - t_0)$, and $\omega_\oplus$ is the Earth's rotation rate. Finally, the satellite position vector in the ECEF coordinate system is given by

$$r_{\mathrm{ECEF}} = R_3(-\lambda_\Omega)R_1(-i)\begin{pmatrix} r\cos u\\ r\sin u\\ 0\end{pmatrix} \tag{12}$$

The equations above form the user algorithm for ephemeris determination. The computational complexity is only slightly more than that of the GPS ephemeris.

Curve fitting

The parameter values of the broadcast ephemeris are generated using a least squares curve fit. A non-singular element set mentioned above is introduced as parameters of the curve fit. In this study, the parameters to be estimated are divided into two groups. One group (X_1) includes 15 compulsory parameters, which corresponds to GPS LNAV ephemeris parameters, and the other group (X_2) is an optional parameter set where the number of parameters varies. Both sets can be summarized as

$$X_1 = \left(\sqrt{a}, i, \Omega, e_x, e_y, \lambda, \Delta n, \dot{\Omega}, \dot{i}, Cus2, Cuc2, Crs2, Crc2, Cis2, Cic2\right)$$

$$X_2 = \left(Cus1, Cuc1, Crs1, Crc1, Cis1, Cic1, Cus3, Cuc3, Crs3, Crc3, Cis3, Cic3, \dot{a}, \dot{n}, \ddot{a}, \ddot{n}, \dot{i}, \ddot{\Omega}\right)$$

We will select, respectively, two, four, and six parameters from X_2 to study.

Compared to the GPS ephemeris parameters, only e, ω, and M are substituted by three non-singular elements (e_x, e_y, λ) for removing the singularity in the curve fit. The partial derivatives of the satellite ECEF position vector with respect to the non-singular elements can be expressed as follows,

$$\begin{aligned}\frac{\partial \boldsymbol{r}}{\partial e_x} &= \left(\frac{\partial \boldsymbol{r}}{\partial \boldsymbol{r}_{\mathrm{ECI}}}\right)\left(\frac{\partial \boldsymbol{r}_{ECI}}{\partial e_x}\right) = R_3(\Theta)\cdot(A\cdot\boldsymbol{r}_{\mathrm{ECI}} + B\cdot\dot{\boldsymbol{r}}_{\mathrm{ECI}})\\ \frac{\partial \boldsymbol{r}}{\partial e_y} &= \left(\frac{\partial \boldsymbol{r}}{\partial \boldsymbol{r}_{\mathrm{ECI}}}\right)\left(\frac{\partial \boldsymbol{r}_{\mathrm{ECI}}}{\partial e_y}\right) = R_3(\Theta)\cdot(C\cdot\boldsymbol{r}_{\mathrm{ECI}} + D\cdot\dot{\boldsymbol{r}}_{\mathrm{ECI}})\\ \frac{\partial \boldsymbol{r}}{\partial \lambda} &= \left(\frac{\partial \boldsymbol{r}}{\partial \boldsymbol{r}_{\mathrm{ECI}}}\right)\left(\frac{\partial \boldsymbol{r}_{\mathrm{ECI}}}{\partial \lambda}\right) = R_3(\Theta)\cdot\frac{\dot{\boldsymbol{r}}_{\mathrm{ECI}}}{n}\end{aligned} \tag{13}$$

where $\boldsymbol{r}_{\mathrm{ECI}}$ and $\dot{\boldsymbol{r}}_{\mathrm{ECI}}$ are the satellite position and velocity vectors in the Earth-centered inertial (ECI) coordinate system. The coefficients A, B, C, and D are given by

$$\begin{aligned}A &= \frac{a}{p}\left[-(\cos u + e_x) - \frac{r}{p}(\sin u + e_y)(e_x\sin u - e_y\cos u)\right]\\ B &= \frac{ar}{\sqrt{GM_\oplus\cdot p}}\left[\sin u + \frac{ae_y\sqrt{1-e^2}}{r(1+\sqrt{1-e^2})} + \frac{r}{p}(\sin u + e_y)\right]\\ C &= -\frac{a}{p}\left[(\sin u + e_y) - \frac{r}{p}(\cos u + e_x)(e_x\sin u - e_y\cos u)\right]\\ D &= -\frac{ar}{\sqrt{GM_\oplus\cdot p}}\left[\cos u + \frac{ae_x\sqrt{1-e^2}}{r(1+\sqrt{1-e^2})} + \frac{r}{p}(\cos u + e_x)\right]\end{aligned} \tag{14}$$

where $p = a(1 - e^2)$ and $r = \sqrt{\boldsymbol{r}\cdot\boldsymbol{r}}$.

After solving the e_x, e_y and λ, they are then transformed to Kepler elements using (2). The partial derivatives of other parameters can be derived from the user algorithm (Cui 2006).

Results

To establish a set of suitable broadcast ephemeris parameters for LEO with consideration of fit accuracy, fit interval, number of parameters, and orbital altitude, an experiment fitting different altitudes of LEOs is carried out. The satellite orbits of 400–1400 km altitudes are simulated using the Positioning And Navigation Data Analyst (PANDA) software (Liu

and Ge 2003). The eccentricity and inclination of all orbits are about 0.001° and 55°. In order to propagate high-precision orbits, the force models, including the geopotential (EIGEN-6C model with 120 degrees and orders), solar and lunar gravitation, atmospheric drag, solar radiation pressure, tides, and relativistic effects are considered. In this section, we compare the fit results for different orbital altitudes and select optimal parameters according to the fit accuracy, which is described by the URE.

LEO URE computation

The impact of orbit errors $\Delta \boldsymbol{r} = (\Delta A, \Delta C, \Delta R)$ in the along-track (ΔA), cross-track (ΔC), and radial (ΔR) directions on the user varies with orientation of the line-of-sight vector and user location. Considering the average contribution over all points of the Earth within the visibility cone of the satellite, the orbit-only contribution to the URE can be described as a weighted average of the RMS errors $A = \mathrm{RMS}(\Delta A)$, $C = \mathrm{RMS}(\Delta C)$, and $R = \mathrm{RMS}(\Delta R)$, as follows

$$\mathrm{URE} = \sqrt{w_R^2 \cdot R^2 + w_{A,C}^2 \cdot (A^2 + C^2)} \tag{15}$$

The weight factors w_R and $w_{A,C}$ depend on the orbital altitude and can be computed as described in Chen et al. (2013). For example, the w_R and $w_{A,C}$ values for GPS are 0.98 and 0.141. Table 2 gives the values of w_R and $w_{A,C}$ for LEOs from 400 to 1400 km, which are almost consistent with those provided by Reid et al. (2016). We can find that the contribution of radial direction to the URE decreases with decreasing orbital altitude. At an altitude of 1000 km, the three directions have an almost equal contribution to the URE.

Parameter selection and fit accuracy

The accuracy of the broadcast ephemeris is driven by orbit determination techniques, propagation errors and model fit errors introduced as part of the parameterization. We only discuss the fit error which is used to compute the UREs in this study. The data used here for the estimating the ephemeris parameters last 20 h from 2:00:00 to 22:00:00 on April 1, 2015. The least squares curve fit with the uniform data sample rate of 60 s is performed to determine the broadcast ephemeris parameters. The update interval is set to half of the fit interval. For the fit interval of 20 min, the update interval is 10 min, and thus there are 120 groups of ephemeris records for 20 h of orbit data. The fit errors are obtained by comparing the satellite position derived from the generated broadcast ephemeris with the simulated satellite orbits.

Table 2 URE weight factors w_R and $w_{A,C}$ for different altitudes of LEOs

Orbital altitude (km)	w_R	$w_{A,C}$
400	0.419	0.642
600	0.488	0.617
800	0.540	0.595
1000	0.582	0.575
1200	0.618	0.556
1400	0.648	0.539

The GPS LNAV ephemeris model with 16 parameters is first used for the curve fit. For the orbital altitude of 1000 km, the RMS errors of 20-min fit in the along-track (A), cross-track (C), and radial (R) components are 19.3, 1.7, and 10.9. When the fit interval is increased to 30 min, the RMS errors increase to 50.6, 7.2, and 36.4 for three components, respectively. It is clear that the fit errors in the along-track and radial components are much larger than that in the cross-track component. According to the weight factors listed in Table 2, the UREs of 12.8 and 36.2 cm for 20- and 30-min fit intervals are obtained. For the orbital altitude of 600 km, the UREs of 20- and 30-min fit intervals are 19.1 and 56.2 cm.

On the basis of 16 parameters, extra parameters from the optional set $X_2 = (Cus1, Cuc1, Crs1, Crc1, Cis1, Cic1, Cus3, Cuc3, Crs3, Crc3, Cis3, Cic3, \dot{a}, \dot{n}, \ddot{a}, \ddot{n}, \dddot{i}, \ddot{\Omega})$ are considered for addition to improve the fit accuracy. We refer to the process used in Fu and Wu (2011) to test all the possibilities of parameter selection and compare their fit accuracies. Considering that cosine and sine harmonic pairs should be selected simultaneously and $(\ddot{a}, \ddot{n})$ may be selected only when $(\dot{a}, \dot{n})$ has been selected, there are 12 possible options for adding two parameters. For the case of adding four and six parameters, there are 59 and 158 possible options. For each possibility, the different altitudes of LEOs (400, 600, 800, 1000, 1200, and 1400 km) with fit intervals (10, 20, 30, 40, 50, and 60 min) are processed. Some representative results of the RMS of fit errors and UREs for adding two, four, and six parameters are listed in Table 3. The orbital altitude used for the curve fit is 1000 km. Table 4 lists the corresponding results for 600 km of LEO. The results of GPS 16-parameter model are also given for comparison.

Compared to GPS 16-parameter model, the first-order and third-order harmonic correction terms to the argument of latitude (u) and the radius (r) affect the fit accuracy in both along-track and radial directions, but not cross-track direction. In the case of adding only two parameters, the $(Cus1, Cuc1)$ and $(Crs1, Crc1)$ show the same effect and have a greater impact on the along-track direction. The $(Cus3, Cuc3)$ shows slight better results than $(Cus1, Cuc1)$ and $(Crs1, Crc1)$ in the along-track direction, but the same results in the radial direction. The minimum fit errors in three directions and the fit UREs are obtained by adding $(Crs3, Crc3)$. The semimajor axis rate ($\dot{a}$) and mean motion

Table 3 Typical results of RMS of the fit errors in the along-track (A), cross-track (C), and radial (R) components as well as the fit UREs with 20- and 30-min fit intervals for a 1000-km LEO

Number of parameters	Additional parameters	20 min (cm)				30 min (cm)			
		A	C	R	URE	A	C	R	URE
16	–	19.3	1.7	10.9	12.8	50.6	7.2	36.4	36.2
18	$\dot{a}, \dot{n}$	7.6	1.7	3.9	5.0	28.5	7.2	17.8	19.8
	$Cus1, Cuc1$	2.9	1.7	8.3	5.2	12.7	7.2	28.6	18.6
	$Crs1, Crc1$	2.9	1.7	8.3	5.2	12.7	7.2	28.6	18.6
	Crs3, Crc3	**2.5**	**1.7**	**4.1**	**3.0**	**11.3**	**7.2**	**15.4**	**11.8**
	$Cus3, Cuc3$	2.5	1.7	8.3	5.1	10.9	7.2	28.6	18.3
20	$\dot{a}, \dot{n}, \ddot{a}, \ddot{n}$	3.6	1.7	1.7	2.5	15.6	7.2	9.4	11.3
	$Cus3, Cuc3, \dot{a}, \dot{n}$	1.2	1.7	3.4	2.3	5.9	7.2	15.2	10.3
	Crs3, Crc3, $\dot{\mathbf{a}}$, $\dot{\mathbf{n}}$	**1.1**	**1.7**	**2.2**	**1.7**	**5.6**	**7.2**	**8.9**	**7.4**
	$Crs3, Crc3, Cus1, Cuc1$	2.9	1.7	1.4	2.1	12.7	7.2	7.2	9.4
	$Crs3, Crc3, Cus3, Cuc3$	3.1	1.7	1.5	2.2	13.2	7.2	8.2	9.9
22	$Crs3, Crc3, \dot{a}, \dot{n}, Cus1, Cuc1$	1.4	1.7	0.9	1.4	7.1	7.2	4.5	6.4
	$Crs3, Crc3, \dot{a}, \dot{n}, Cis3, Cic3$	1.1	0.3	2.2	1.4	5.6	1.9	8.9	6.2
	Crs3, Crc3, $\dot{\mathbf{a}}$, $\dot{\mathbf{n}}$, $\ddot{\mathbf{i}}$, $\ddot{\mathbf{a}}$	**1.2**	**0.7**	**1.1**	**1.0**	**6.2**	**3.7**	**5.6**	**5.3**
	$Crs3, Crc3, \dot{a}, \dot{n}, \ddot{i}, \ddot{\Omega}$	1.1	0.4	2.2	1.4	5.6	2.2	8.9	6.2

The parts in bold achieve the minimum fit UREs for the same number of parameters

Table 4 Typical results of RMS of the fit errors with 16-, 18-, 20-, and 22-parameter models for a 600-km LEO

Number of parameters	Additional parameters	20 min (cm)				30 min (cm)			
		A	C	R	URE	A	C	R	URE
16	–	26.9	4.3	18.4	19.1	75.7	16.4	60.5	56.2
18	$\dot{a}, \dot{n}$	16.7	4.3	8.8	11.5	47.0	16.4	33.2	34.7
	$Cus1, Cuc1$	6.4	4.3	15.3	8.8	24.0	16.4	49.3	30.0
	$Crs1, Crc1$	6.4	4.3	15.3	8.8	24.0	16.4	49.3	30.0
	Crs3, Crc3	**5.5**	**4.3**	**9.4**	**6.3**	**21.5**	**16.4**	**28.7**	**21.8**
	$Cus3, Cuc3$	5.9	4.3	15.3	8.7	21.0	16.4	49.3	29.1
20	$\dot{a}, \dot{n}, \ddot{a}, \ddot{n}$	7.5	4.3	4.4	5.7	28.9	16.4	19.5	22.6
	$Cus3, Cuc3, \dot{a}, \dot{n}$	3.1	4.3	7.6	4.9	12.3	16.4	28.8	18.9
	Crs3, Crc3, $\dot{\mathbf{a}}$, $\dot{\mathbf{n}}$	**2.8**	**4.3**	**5.1**	**4.0**	**11.7**	**16.4**	**17.9**	**15.2**
	$Crs3, Crc3, Cus1, Cuc1$	6.4	4.3	3.8	5.1	24.0	16.4	15.4	19.5
	$Crs3, Crc3, Cus3, Cuc3$	6.9	4.3	4.2	5.4	24.9	16.4	17.3	20.2
22	$Crs3, Crc3, \dot{a}, \dot{n}, Cus1, Cuc1$	3.2	4.3	2.4	3.5	13.5	16.4	9.6	13.9
	$Crs3, Crc3, \dot{a}, \dot{n}, Cis3, Cic3$	2.8	1.2	5.1	3.1	11.7	5.3	17.9	11.8
	Crs3, Crc3, $\dot{\mathbf{a}}$, $\dot{\mathbf{n}}$, $\ddot{\mathbf{i}}$, $\ddot{\mathbf{a}}$	**3.1**	**2.4**	**3.2**	**2.9**	**12.7**	**9.9**	**12.5**	**11.7**
	$Crs3, Crc3, \dot{a}, \dot{n}, \ddot{i}, \ddot{\Omega}$	2.8	1.3	5.1	3.1	11.7	6.0	17.9	11.9

The parts in bold achieve the minimum fit UREs for the same number of parameters

rate ($\dot{n}$) have no effect on cross-track direction as well. The fit accuracy in cross-track direction is only affected by the corrections to inclination (i) and RAAN (Ω), such as ($\ddot{i}, \ddot{\Omega}$) and ($Cis3, Cic3$). In addition, the optimal situations in terms of the fit accuracy are the same for 1000- and 600-km LEOs. For the cases of adding four and six parameters, the optimal selections are ($Crs3, Crc3, \dot{a}, \dot{n}$) and ($Crs3, Crc3, \dot{a}, \dot{n}, \ddot{i}, \ddot{a}$). It should be noted that the 18-, 20-, and 22-parameter models mentioned below refer in particular to the situations of optimal selections for adding two, four, and six parameters, i.e., ($Crs3, Crc3$),($Crs3, Crc3, \dot{a}, \dot{n}$) and ($Crs3, Crc3, \dot{a}, \dot{n}, \ddot{i}, \ddot{a}$).

As an example, Fig. 2 shows the time series of fit errors for the 20-parameter model and 1000 km of orbit. For the fit interval of 20 min, the fit errors in all three components are staying within ± 8 cm, and the UREs are better than 6 cm. For the fit interval of 30 min, the fit errors in the three components vary within ± 20 cm, and the UREs are better than 20 cm. The RMS values of the fit UREs for 20- and 30-min fit intervals are 1.7 and 7.4 cm, respectively.

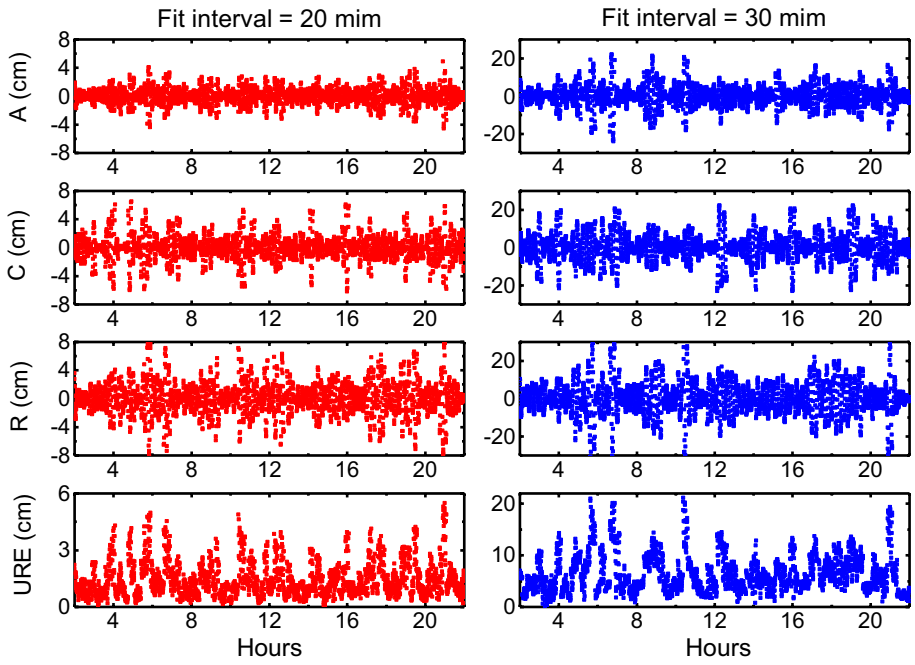

Fig. 2 Fit errors in the along-track (*A*), cross-track (*C*), and radial (*R*) components as well as the fit UREs with a 20-parameter model for a 1000-km LEO. The panels on the left and the right represent the results of 20- and 30-min fit intervals for 20 h of orbit data, respectively

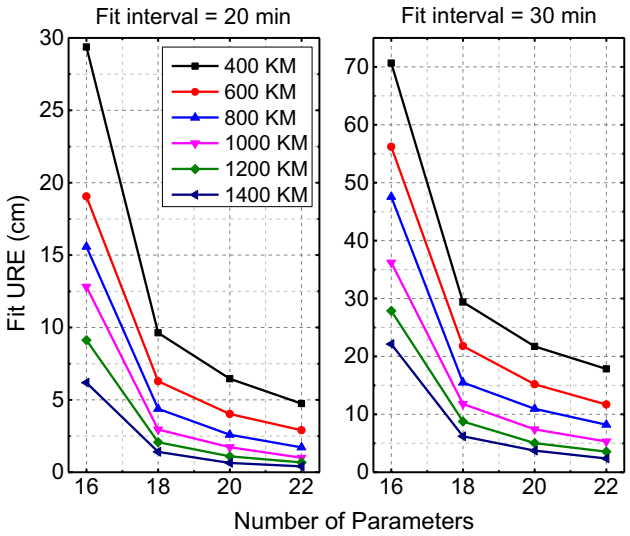

Fig. 3 Fit UREs for LEOs of 400–1400 km altitude as a function of the number of model parameters, with fit intervals of 20 min (left) and 30 min (right)

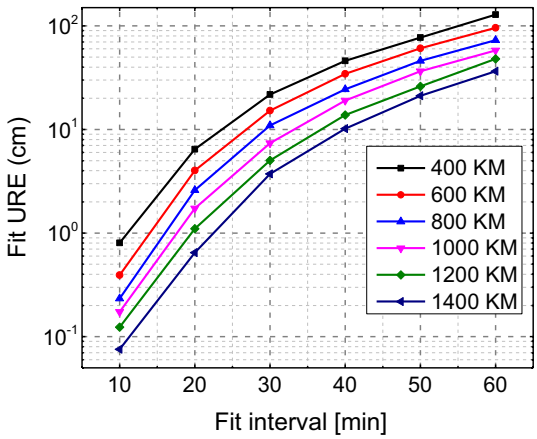

Fig. 4 Fit UREs of 20-parameter model for LEOs of 400–1400 km altitude as a function of the fit intervals

Discussion

The LEO fit accuracy is mainly affected by the fit interval, the number of parameters of the broadcast ephemeris model, and the orbital altitude, which are investigated in this section. Moreover, the proposed models are validated and compared by typical satellites in orbit.

Impact analysis of fit accuracy

Figure 3 shows the relationship between the fit UREs and the number of model parameters for different altitudes of LEOs. It is obvious that the fit UREs are dramatically reduced with the increase in the number of parameters, especially for the situation of the 18-parameter compared to the 16-parameter model. This is mainly due to the improvement in the fit accuracy in the along-track and radial components (Tables 3, 4). Due to a small reduction in the magnitude of

UREs compared to the 22-parameter model, it is reasonable to select 20-parameter for LEOs broadcast ephemeris model. In addition, the orbital altitude has a significant effect on the fit accuracy. The fit UREs increase with the decrease in the orbital altitude when the same fit interval and parameter number are used.

Figure 4 shows the relationship between the fit UREs and the fit interval for different altitudes of LEOs. The 20-parameter model is used. We can see that the fit UREs significantly increase with the increasing fit intervals. The fit UREs smaller than 1 cm can be achieved with 10-min fit interval for all orbits, while the values reach up to 30–130 cm for 60-min fit interval. To achieve the fit UREs of better than 10 cm, the fit intervals of 400, 600, 800, 1000, 1200, and 1400 km orbits should be less than about 24, 27, 30, 33, 37, and 40 min, respectively. These intervals are greatly extended compared to that of the GPS 16-parameter model.

Validation of real orbits

The four LEO satellites in orbit, named GRACE-A, CryoSat-2, HY-2A, and Jason-2, with an orbital altitude of about 485–1336 km are selected to validate the proposed broadcast ephemeris model. The precise orbit products of these satellites are used for the broadcast ephemeris curve fit experiment. Table 5 lists some basic orbit information of these satellites. The eccentricities of these orbits are close or equal to zero.

Figure 5 shows the fit URE time series of the HY-2A orbit for 16-, 18-, 20-, and 22-parameter models with 20-min fit interval. It is found that the improvement in the fit accuracy is very significant by adding a few appropriate parameters. The RMS values of the fit UREs are, respectively, 11.5, 3.6, 2.1, and 1.2 for the four models. Given the orbital altitude of 971 km, these values are approximately equal to the results of the aforementioned simulated orbit of 1000 km in Table 3, which are 12.8, 3.0, 1.7, and 1.0, respectively.

Similar to Fig. 4, Fig. 6 illustrates the relationship between the fit UREs and the fit interval for the selected four LEOs. Similar results can be seen. Moreover, for the similar orbital altitude as shown in Fig. 4, the fit UREs with the same intervals are approximately the same. Although the eccentricities of CryoSat-2 and Jason-2 are zero, the solutions of the least squares curve fit are successful. This demonstrates that our fit algorithm based on the used non-singular elements is reliable and suitable for LEOs.

Table 5 Basic orbit information for satellites used for broadcast ephemeris validation

Satellite Name	Altitude (km)	Inclination (°)	Eccentricity
GRACE-A	485–500	89	< 0.005
CryoSat-2	720	92	0.000
HY-2A	971	99.35	0.00117
Jason-2	1336	66	0.000

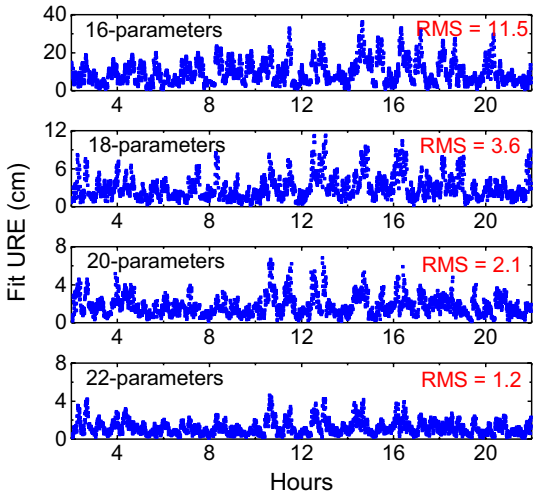

Fig. 5 Time series of fit UREs for the HY-2A satellite orbit for 16-, 18-, 20-, and 22-parameter models with 20-min fit interval

Conclusions

Compared to MEO, IGSO, and GEO satellites, a LEO satellite has a very short orbital period and more complex orbital dynamics, which increase the difficulty for high-precision orbital representation. We presented a model design of LEO broadcast ephemeris based on the standard GPS ephemeris model. The non-singular elements are introduced as parameters to eliminate the singularity caused by the small eccentricity of LEO satellites. Analysis of the characteristics of

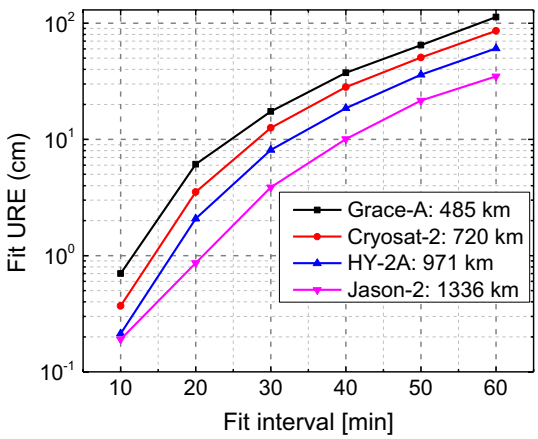

Fig. 6 Fit UREs of 20-parameter model as a function of the fit intervals for four LEO satellites in orbit

the orbital perturbations suggests specific parameters should be considered as candidates that are added on the GPS 16 parameters.

The fit accuracy of different parameter selections has been compared, and optimal selections have been determined. The results suggest that ($Crs3, Crc3$), ($Crs3, Crc3, \dot{a}, \dot{n}$) and ($Crs3, Crc3, \dot{a}, \dot{n}, \ddot{i}, \ddot{a}$) for adding two, four and six parameters can achieve the minimum fit errors. When adding four parameters ($Crs3, Crc3, \dot{a}, \dot{n}$), the RMS values of fit UREs reach to 1.7 and 7.4 cm with 20- and 30-min fit intervals for 1000 km of LEO. The effects of the number of parameters, fit interval and orbital altitude on fit accuracy were investigated. The fit UREs are dramatically reduced with the increase in the number of parameters and the orbital altitude, as well as the shortening of the fit intervals. Furthermore, the effectiveness of proposed ephemeris models was validated by the four LEO satellites in orbit at different altitudes.

It is worth noting that we focus mainly on the model fit accuracy and parameter update frequency (fit interval) of LEO broadcast ephemeris. While other aspects, such as the message size, least significant bit, message block structure, and users' time-to-first-fix, are also very important for broadcast ephemeris design of navigation systems, which are considered as an ongoing research effort.

Acknowledgements This work is supported by the National Nature Science Foundation of China (Nos. 41674004, 41574030) and Fundamental Research Funds for the Central Universities (No. 2042016kf0185).

References

Brouwer D, Clemence GM, Chako N (2005) Methods of celestial mechanics. Springer, Berlin

Chen L, Jiao W, Huang X, Geng C, Ai L, Lu L, Hu Z (2013) Study on signal-in-space errors calculation method and statistical characterization of BeiDou navigation satellite system. Proc China Satell Navig Conf 2013:423–434

CSNO (2013) BeiDou navigation satellite system signal in space interface control document-open service signal. Version 2.0, 26 December 2013, China Satellite Navigation Office (CSNO)

Cui X (2006) Comparisons of two kinds of GPS broadcast ephemeris parameter algorithms. Chin J Sp Sci 26(5):382–387

Dierendonck AJV, Russell SS, Kopitzke ER, Birnbaum M (1978) The GPS navigation message. Navigation 25(2):147–165

Diesposti R, Dilellio J, Kelley C, Dorsey A, Fliegel H, Berg J, Edgar C, Mckendree T, Shome P (2004) The proposed state vector representation of broadcast navigation message for user equipment implementation of GPS satellite ephemeris propagation. In: Proceedings of the ION NTM 2004, pp 294–312. Institute of Navigation, San Diego, California, USA, 26–28 Jan

Du L, Zhang Z, Zhang J, Liu L, Guo R, He F (2014) An 18-element GEO broadcast ephemeris based on non-singular elements. GPS Solut 19(1):49–59

EU (2015) European GNSS (Galileo) open service signal in space interface control document. Issue 1.2, November 2015. European Union

Fang S, Du L, Zhou P, Lu Y, Zhang Z, Liu Z (2016) Orbital list ephemerides design of LEO navigation augmentation satellite. Acta Geod Cartogr Sin 45(8):904–910

Fu X, Wu M (2011) Optimal design of broadcast ephemeris parameters for a navigation satellite system. GPS Solut 16(4):439–448

Gilthorpe MS, Moore P (1992) A combined theory for zonal harmonic and resonance perturbations of a near-circular orbit with applications to COSMOS 1603 (1984-106A). Celest Mech Dyn Astron 54(4):363–391

GPS Directorate (2013) Navstar GPS space segment/navigation user interfaces. Interface specification, IS-GPS-200H, Version H, September 23, 2013, Global Positioning Systems Directorate

Guo J, Zhao Q, Guo X, Liu X, Liu J, Zhou Q (2015) Quality assessment of onboard GPS receiver and its combination with DORIS and SLR for Haiyang 2A precise orbit determination. Sci China Earth Sci 58(1):138–150

He F, Hu X, Liu L, Huang H, Zhou S, Wu S, Gu L, Zhao H, Liu X (2014) Fitting method and accuracy analysis of broadcast ephemeris in hybrid constellation. Proc China Satell Navig Conf 2014:265–275

Heng L, Gao G, Walter T, Enge P (2011) Statistical characterization of GLONASS broadcast ephemeris errors. In: Proceedings of the ION GNSS 2011, pp 3109–3117. Institute of Navigation, Portland, Oregon, USA, 19–23 Sept

Hintz GR (2008) Survey of orbit element sets. J Guid Control Dyn 31(3):785–790

Horemuž M, Andersson JV (2006) Polynomial interpolation of GPS satellite coordinates. GPS Solut 10(1):67–72

Hu Z, Chen G, Zhang Q, Guo J, Su X, Li X, Zhao Q, Liu J (2013) An initial evaluation about BDS navigation message accuracy. Proc China Satell Navig Conf 2013:479–491

Hugentobler U, Montenbruck O (2017) Satellite orbits and attitude, Chap. 3. In: Teunissen PJG, Montenbruck O (eds) Springer handbook of global navigation satellite systems. Springer, Berlin

ICD-GLONASS (2016) Global navigation satellite system GLONASS, interface control document, general description of code division multiple access signal system. Edition 1.0, Russian Institute of Space Device Engineering

JAXA (2014) Quasi-Zenith satellite system navigation service interface specification for QZSS. IS-QZSS V1.6, November 28, 2014, Japan Aerospace Exploration Agency

Joerger M, Neale J, Pervan B (2009) Iridium/GPS carrier phase positioning and fault detection over wide areas. In: Proceedings of the ION GNSS 2009, pp 1371–1385. Institute of Navigation, Savannah, Georgia, USA, 22–25 Sept

Joerger M, Gratton L, Pervan B, Cohen CE (2010) Analysis of iridium-augmented GPS for floating carrier phase positioning. Navigation 57(2):137–160

Liu J, Ge M (2003) PANDA software and its preliminary result of positioning and orbit determination. Wuhan Univ J Nat Sci 8(2B):603–609

Montenbruck O, Gill E (2000) Satellite orbits: models, methods, and applications. Springer, Berlin

Montenbruck O, Steigenberger P, Hauschild A (2014) Broadcast versus precise ephemerides: a multi-GNSS perspective. GPS Solut 19(2):321–333

Piscane VL, Holland BB, Black HD (1973) Recent (1973) improvements in the navy navigation satellite system. Navigation 20(3):224–229

Rabinowitz M, Spilker JJ (2005) A new positioning system using television synchronization signals. IEEE Trans Broadcast 51(1):51–61

Reid TGR, Walter T, Enge PK, Sakai T (2015) Orbital representations for the next generation of satellite-based augmentation systems. GPS Solut 20(4):737–750

Reid TGR, Neish A, Walter T, Enge PK (2016) Leveraging commercial broadband LEO constellations for navigation. In: Proceedings of

the ION GNSS + 2016, pp 2300–2314. Institute of Navigation, Portland, Oregon, USA, 12–16 Sept
Thomas A, Stansell JR (1968) The navy navigation satellite system: description and status. Navigation 15(3):229–243
Tian S, Dai W, Liu R, Chang J, Li G (2014) System using hybrid LEO-GPS satellites for rapid resolution of integer cycle ambiguities. IEEE Trans Aerosp Electron Syst 50(3):1774–1785
Warren DL, Raquet JF (2003) Broadcast vs. precise GPS ephemerides: a historical perspective. GPS Solut 7(3):151–156
Xu G, Xu Y (2007) GPS: theory, algorithms and applications. Springer, Berlin
Xu G, Xu J (2013) On the singularity problem in orbital mechanics. Mon Not R Astron Soc 429(2):1139–1148
Yin H, Morton Y, Carroll M, Vinande E (2015) Performance analysis of L2 and L5 CNAV broadcast ephemeris for orbit calculation. Navigation 62(2):121–130

Xin Xie is currently a Ph.D. candidate at GNSS Research Center, Wuhan University. He received his B.Sc. degree in 2014 from China University of Geosciences. His research interests include precise orbit determination of GNSS and high-precision positioning using GNSS.

Tao Geng is an associate professor at GNSS Research Center, Wuhan University, China. He received his Ph.D. in Geodesy and Surveying Engineering from Wuhan University in 2009. From February 2013 to February 2014, he was a visiting scholar at Ohio State University. His research interests include precise GNSS orbit determination and positioning.

Qile Zhao is a professor of GNSS Research Center of Wuhan University. He received his Ph.D. degree in Wuhan University in 2004. In 2006–2007, as a postdoctoral fellow, he did his postdoctoral program in DEOS, Delft University of Technology, the Netherlands. His current research interests are precise orbit determination of GNSS and low Earth orbit satellites, and high-precision positioning using GPS, Galileo and BDS system.

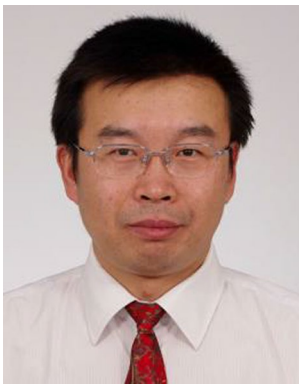

Xianglin Liu is a senior geodesist and the lead of GNSS R&D group at Fugro Intersite B.V., the Netherlands. He received his Ph.D. degrees from Delft University of Technology and Wuhan University. His main research focuses on PPP-RTK with multi-GNSS and multi-frequency observations.

Qiang Zhang is currently a Ph.D. candidate at GNSS Research Center of Wuhan University. He received his bachelor's and master's degrees at Wuhan University in 2011 and 2013, respectively. His current research interests focus on precise orbit determination of low Earth orbiters using space-borne GPS observations only.

Jingnan Liu graduated from the former Wuhan College of Surveying and Mapping in 1967 and received his master's degree in 1982. He was elected Academician of the Chinese Academy of Engineering in 1999. He has been a member of the Science and Technology Committee, Ministry of Education of China in 1997–2009 and as an editorial board member of GPS Solutions in 1998–2000. He is currently an executive member of the council, Chinese Society for Geodesy Photogrammetry and Cartography; the editorial board member of GPS World; and the coordinator of International GPS Geodynamics Services. His current research interests are satellite precise orbit determination.